View metadata, citation and similar papers at core.ac.uk
brought to you by CORE
provided by Electronic Sumy State University Institutional Repository

JOURNAL OF NANO- AND ELECTRONIC PHYSICS
Vol. 4 No 4, 04002(4pp) (2012)
ЖУРНАЛ НАНО- ТА ЕЛЕКТРОННОЇ ФІЗИКИ
Том 4 № 4, 04002(4cc) (2012)

Preparation and Characterization of NiO Thin Films by DC Reactive Magnetron Sputtering

Y. Ashok Kumar Reddy[1], A. Mallikarjuna Reddy[1], A. Sivasankar Reddy[2], P. Sreedhara Reddy[1,*]

[1] *Department of Physics, Sri Venkateswara University, Tirupati 517 502 India*
[2] *Division of Advanced Materials Engineering, Kongju National University, Budaedong, Cheonan City, South Korea*

(Received 06 August 2012; revised manuscript received 20 December 2012; published online 29 December 2012)

Nickel oxide (NiO) thin films were successfully deposited on Corning 7059 glass substrates at different oxygen partial pressures in the range of 1×10^{-4} to 9×10^{-4} mbar using dc reactive magnetron sputtering technique. Structural properties of NiO films showed polycrystalline nature with cubic structure along (220) orientation. The optical transmittance and band gap values of the films increased with increasing the oxygen partial pressure from 1×10^{-4} to 5×10^{-4} mbar and decreased on further increasing the oxygen partial pressure. Using Scanning Electron Microscopy (SEM), fine grains were observed at oxygen partial pressure of 5×10^{-4} mbar. The film resistivity decreases from 90.48 to 13.24 Ω cm with increase in oxygen partial pressure to 5×10^{-4} mbar and then increased on further increasing the oxygen partial pressure.

Keywords: Sputtering, NiO thin films, Structural properties, Optical properties, Electrical properties, Oxygen partial pressure.

PACS numbers: 81.15.Cd, 73.61.Ey

1. INTRODUCTION

Nickel oxide is a transition metal oxide semiconductor, usually taken as a model for p-type material. NiO is having wide band gap of 3.6 to 4.0 eV [1] and exhibit rhombohedral or cubic structure, but the most prominent structure was cubic structure [2]. NiO thin films have been studied for applications in electrochromic devices [3], electrode material for Li-ion batteries [4]. Recent works have shown that NiO is also a promising functional material for applications in resistive type gas sensors implementing thin NiO films [5, 6]. Most attractive features of NiO are: (i) excellent durability and electrochemical stability, (ii) low materials cost, (iii) promising ion storage material in terms of cyclic stability, (iv)large spin optical density and (v) possibility of manufacturing by variety of techniques. NiO films can be prepared by physical and chemical methods such as: spray pyrolysis [7], electron beam evaporation [8], pulsed laser deposition [9], plasma enhanced chemical vapor deposition [10] and reactive sputtering [11]. It is well known that the structural, optical, surface morphology and electrical properties of materials in thin film form depends on the deposition conditions like oxygen partial pressure. Recently, our research group [12] reported the NiO films by using dc magnetron sputtering with various oxygen partial pressures. In this study, an attempt was made on the fabrication of NiO films at different deposition conditions (like pO_2, substrate temperature and target to substrate distance comparing to earlier paper) for enhancing the physical properties.

We have successfully deposited NiO thin films by dc reactive magnetron sputtering from a metallic Ni target in a mixture of oxygen and argon. In this paper we have investigated the structural, optical, Surface morphology, chemical and electrical studies of direct current sputter deposited highly oriented NiO thin films as a function of oxygen partial pressure.

2. EXPERIMENTAL DETAILS

2.1 Preparation of NiO Thin Films

NiO films were deposited from a pure nickel (99.98 %) target (100 mm diameter and 3 mm thickness) in a mixture of oxygen and argon gases on Corning 7059 glass substrates by using dc reactive magnetron sputtering system. In the present study, NiO thin films were deposited at various oxygen partial pressures by keeping the other depositions conditions such as substrate temperature, sputtering power, sputtering pressure and target to substrate distance are constant. The deposition parameters are used during the formation of NiO thin films were given in Table 1.

Table 1 – Deposition parameters of NiO films

№	Deposition conditions	Range
1	Target-substrate distance	75 mm
2	Ultimate pressure	5×10^{-6} mbar
3	Oxygen partial pressure	1×10^{-4}-9×10^{-4}mbar
4	Sputtering pressure	2×10^{-3} mbar
5	Substrate temperature	473 K
6	Sputtering power	90 W
7	Deposition time	10 min

2.2 Characterization Techniques

The structure of the deposited films were analyzed by X-ray diffractometer using Cu Kα radiation ($\lambda = 0.1546$ nm) of model 3033TT manufactured by Seifert, the optical transmittance studied using Perkin Elmer Lambda 950 UV-Vis-NIR spectrophotometer and the surface morphology was studied by scanning electron microscope (SEM) of model EVO MA 15 manufactured by Carl Zeiss. The chemical composition of the films were examined by Energy Dispersive Spectroscopy (EDS) attached with SEM of model Oxford instruments Inca Penta FET x 3. The electrical properties were performed by using an Ecopia Hall effect measurement system (HMS-3000VER 3.51.3).

* psreddy4@gmail.com

© 2012 Sumy State University

3. RESULTS AND DISCUSSION

3.1 Structural Properties

The X-ray diffraction patterns of the deposited NiO films at various oxygen partial pressures were shown in Fig. 1. The films were identified to be polycrystalline nature with cubic structure along (220) orientation (JCPDS card no.78-0643). As the oxygen partial pressure increased to 5×10^{-4} mbar, the intensity of (220) peak was increased and becomes sharper. Beyond this oxygen partial pressure, the intensity of (220) peak was gradually decreased. The increased intensity of (220) peak may be due to an increase in the crystallite size and further the decrease in the intensity of (220) peak due to excess oxygen segregation at the grain boundaries [13].

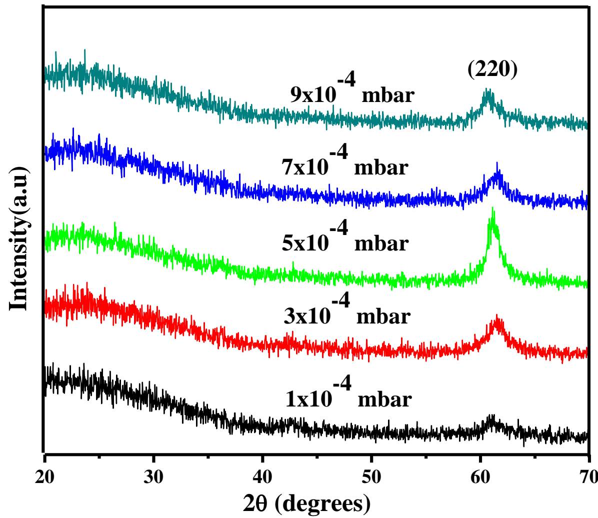

Fig. 1 – X-ray diffraction profiles of NiO films at various oxygen partial pressures

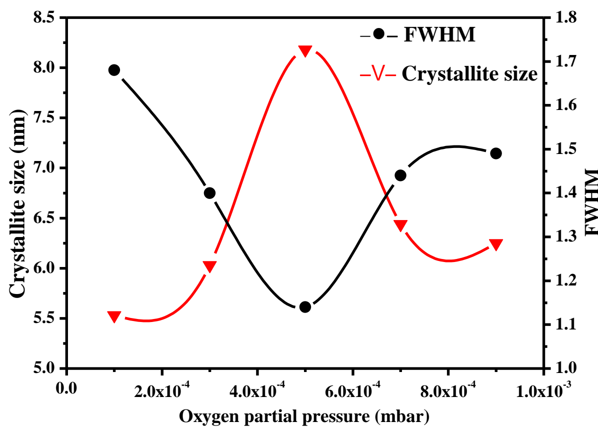

Fig. 2 – The behavior of crystallite size and FWHM of NiO thin films deposited at various oxygen partial pressures

The crystallite size of the films was calculated from the (220) orientation by using Scherrer formula [14].

$$L = K\lambda / \beta\cos\theta, \quad (3.1)$$

Where L is the mean crystallite size, K is the correction factor, λ is the wavelength of the incident beam, β is the full width at half maximum corresponding to Bragg diffraction angle θ. Here K, λ values taken as 0.94 and 0.1541 nm respectively. The crystallite size of the films increased from 5.6 to 8.2 nm with increase of oxygen partial pressure from 1×10^{-4} to 5×10^{-4} mbar, thereafter it was decreased to 6.3 nm at higher oxygen partial pressures. Fig. 2 shows the full width at half maximum (FWHM) and the crystallite size as a function of oxygen partial pressure.

3.2 Optical Properties

The optical transmittance spectra of the deposited NiO films at various oxygen partial pressures were shown in Fig. 3. The optical transmittance of the films increased from 29 % to 40 % with increasing oxygen partial pressure from 1×10^{-4} to 5×10^{-4} mbar. On further increasing the oxygen partial pressure to 9×10^{-4} mbar the transmittance of the films decreased to 34 %, which was due to the defects of non-stoichiometric NiO thin films. The optical absorption coefficient (α) was calculated from the optical transmittance (T) and reflectance (R) data using the relation

$$\alpha = 1/t\ [\ln T / (1 - R^2)] \quad (3.2)$$

where, t is the thickness of the films.

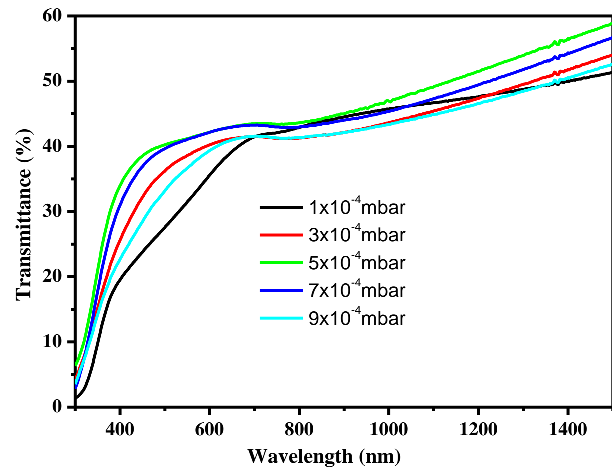

Fig. 3 – Optical transmittance spectra of NiO films as a function of oxygen partial pressure

The dependence of α on the photon energy ($h\nu$) fitted to the relation for direct transition

$$\alpha h\nu = A\,(h\nu - E_g)^{1/2} \quad (3.3)$$

where, E_g is the band gap of the films.

The plots of $(\alpha h\nu)^2$ versus photon energy ($h\nu$) of the NiO films formed at various oxygen partial pressures were shown in Fig. 4. The optical band gap of the films increased from 3.01 to 3.6 eV with increase in oxygen partial pressure from 1×10^{-4} to 5×10^{-4} mbar, beyond this oxygen partial pressure the band gap decreased to 3.08 eV. However in the literature, large optical band gap of 4.3 eV was reported by Romero et al [15] in chemical spray pyrolysis deposited NiO films.

Table 2 – Optical information of dc reactive magnetron sputtered NiO films at various oxygen partial pressures

№	Oxygen partial Pressure (mbar)	Transmittance (%)	Optical band gap (eV)
1	1×10^{-4}	29	3.02
2	3×10^{-4}	35	3.30
3	5×10^{-4}	40	3.60
4	7×10^{-4}	39	3.40
5	9×10^{-4}	34	3.08

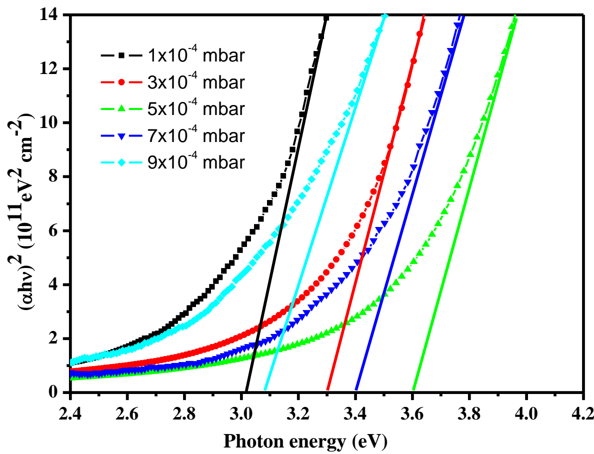

Fig. 4 – Plots of $(\alpha h\nu)^2$ versus $(h\nu)$ of NiO at various oxygen partial pressures

3.3 Morphological and Compositional Analysis

The scanning electron microscopy (SEM) images of NiO films deposited at various oxygen partial pressures were shown in Fig. 5. At an oxygen partial pressure 1×10^{-4} mbar, it was observed that very smooth surface and the fine grains were appeared when the films deposited at an oxygen partial pressure of 5×10^{-4} mbar. When the films deposited beyond this oxygen partial pressure the number of the grains decreased. At higher oxygen partial pressures, the surface mobility of the adatoms decreased due to excess oxygen, resulting the decrease in number of grains.

The Energy Dispersive Spectroscopy (EDS) was employed to identify the composition of the as deposited NiO films at different oxygen partial pressures. Fig. 6 shows the typical EDS spectra of NiO films deposited at 5×10^{-4} mbar oxygen partial pressure. EDS results revealed that all the deposited films consist of nickel and oxygen. The composition of nickel decreased with increasing oxygen partial pressure due to increase in the oxygen concentration.

3.4 Electrical Properties

The resistivity of NiO films was measured by Hall-effect. The resistivity ρ is inversely proportional to the product of carrier concentration N and mobility μ as the following relation [16]:

$$\rho = 1 / Ne\mu \qquad (3.4)$$

where, e is the electric charge. It was found that the resistivity of the NiO films decreased from 90.48 to 13.24 Ω cm with the increase in oxygen partial pressure

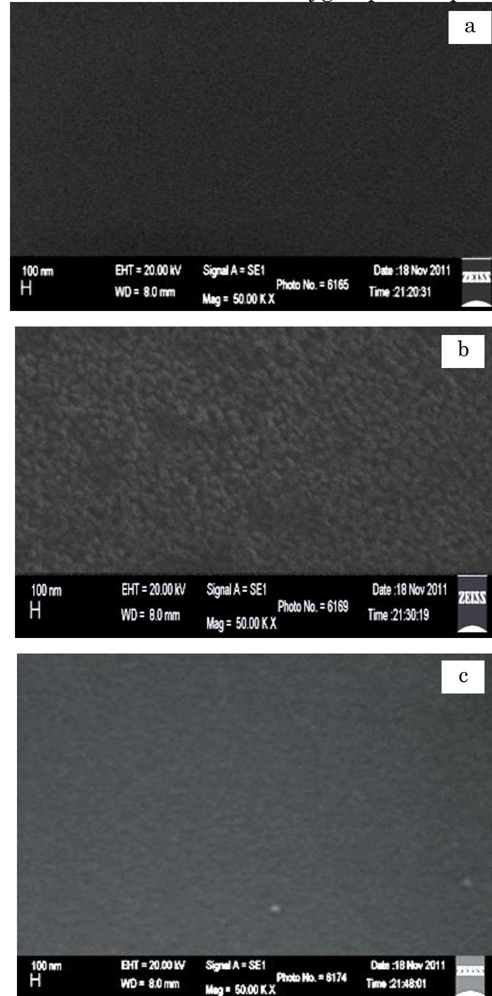

Fig. 5 – SEM images of NiO films at different oxygen partial pressures: 1×10^{-4} mbar (a), 5×10^{-4} mbar (b), 1×10^{-3} mbar (c)

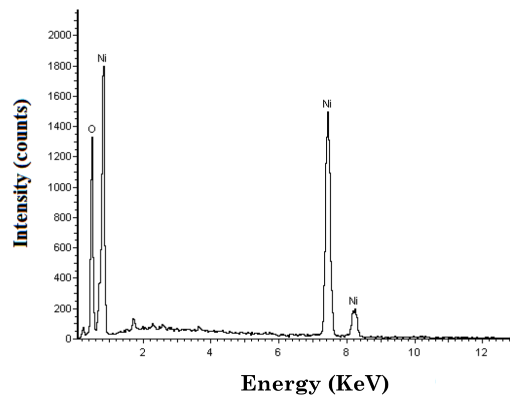

Fig. 6 – Typical EDS profile of NiO films at 5×10^{-4} mbar oxygen partial pressures

to 5×10^{-4} mbar, and then increased to 59.42 Ω cm at higher oxygen partial pressure of 9×10^{-4} mbar. The decrease in resistivity with the oxygen partial pressure was related to increase in the crystallinity of the films. On increasing the oxygen partial pressure from 1×10^{-4} to 5×10^{-4} mbar, the carrier concentration of the films increased from 6.2×10^{16} to 8.4×10^{18} cm^{-3}. We observed that all carrier concentration values are positive in the NiO films, which indicates that the films exhibit

p-type conduction. The Hall mobility of the films increased from 0.9 to 4.5 $cm^2V^{-1}s^{-1}$ with the increase in oxygen partial pressure to 5×10^{-4} mbar, thereafter it was decreased to 2.8 $cm^2V^{-1}s^{-1}$ at higher oxygen partial pressures. The mobility value was low due to collisional energy loss of the particles with oxygen during their arrival towards the substrate surface [17]. Fig. 7 shows that the behavior of resistivity, carrier concentration and mobility of the films at different oxygen partial pressures.

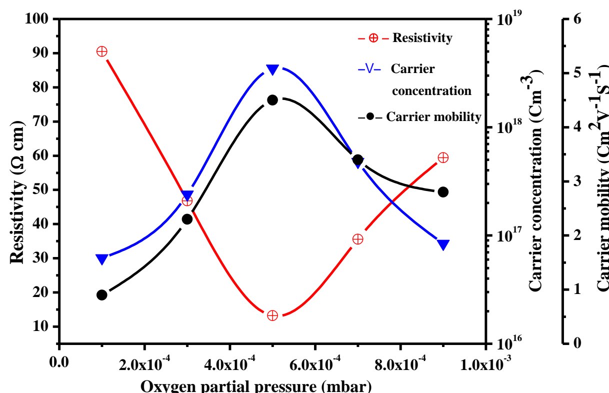

Fig. 7 – Behaviour of resistivity, mobility and carrier concentration of NiO thin films as a function of oxygen partial pressure

4. CONCLUSIONS

The p-type NiO films were successfully deposited by dc reactive magnetron sputtering at different oxygen partial pressures. NiO films exhibited polycrystalline nature with cubic structure along (220) orientation. The optical transmittance and band gap of the films increased with increasing the oxygen partial pressure from 1×10^{-4} to 5×10^{-4} mbar and decreased at higher oxygen partial pressures. In Scanning Electron Microscopy (SEM) analysis fine grains were observed at oxygen partial pressure of 5×10^{-4} mbar, beyond this oxygen partial pressure the number of grains was decreased. The electrical resistivity values shows in decreasing tendency up to oxygen partial pressure of 5×10^{-4} mbar and then increased.

ACKNOWLEDGMENTS

The authors are very thankful to the University Grants Commission (UGC), New Delhi (File No. F.40-419/2011(SR)) for providing the financial assistance to carry out the above work.

REFERENCES

1. H.J.M. Swagten, G.J. Strijkers, P.J.H. Bloemen, M.M.H. Willekens, W.J.M. De Jonge, *Phys. Rev. B* **53**, 9108 (1996).
2. K.K. Purushothaman, G. Muralidharan, *Sol. Energ. Mat. Sol. C.* **93**, 1195 (2009).
3. Zhang Xuping, Chen Guoping, *Thin Solid Films* **298**, 53 (1997).
4. Ying Wang, Ya-Fei Zhang, Hai-Rong Liu, Shen-Jiang Yu, Qi-Zong Qin, *Electrochim. Acta* **48**, 4253 (2003).
5. I. Hotovy, J. Huran, P. Siciliano, S. Capone, L. Spiess, V. Rehacek, *Sensor. Actuat. B-Chem.* **103**, 300 (2004).
6. I. Hotovy, J. Huran, L. Spiess, H. Romanus, D. Buc, R. Kosiba, *Thin Solid Films* **515**, 658 (2006).
7. J.D. Desai, Sun-Ki Min, Kwang-Deog Jung, Oh-Shim Joo, *Appl. Surf. Sci.* **253**, 1781 (2006).
8. A. Agrawal, H.R. Habibi, R.K. Agrawal, J.P. Cronin, D.M. Roberts, C.P. R'Sue, C.M. Lampert, *Thin Solid Films* **221**, 239 (1992).
9. M. Tanaka, M. Mukai, Y. Fujimori, M. Kondoh, Y. Tasaka, H. Baba, S. Usami, *Thin Solid Films* **281**, 453 (1996).
10. W.C. Yeh, M. Matsumura, *Jpn. J. Appl. Phys.* **36**, 6884 (1997).
11. M. Bönger, A. Fuchs, K. Scharnagl, R. Winter, T. Doll, I. Eisele, *Sensor. Actuat. B-Chem.* **47**, 145 (1998).
12. A. Mallikarjuna Reddy, A. Sivasankar Reddy, Kee-Sun Lee, P. Sreedhara Reddy, *Ceram. Int.* **37**, 2837 (2011).
13. K. Ellmer, *J. Phys. D. Appl. Phys.* **33**, R17 (2000).
14. B.D. Cullity, *Elements of X-ray Diffraction*, second ed., (London: Addison Wesley: 1978).
15. R. Romero, F. Martin, J.R. Ramos-Barrado, D. Leinen, *Thin Solid Films* **518**, 4499 (2010).
16. Y. Igasaki, H. Saito, *Thin Solid Films* **199**, 223 (1991).
17. T.K. Yong, T.Y. Tou, B.S. Teo, *Appl. Surf. Sci.* **248**, 388 (2005).